Characterization of linear interfacial waves in a turbulent gas-liquid pipe flow

A. A. Ayati, P. S. C. Farias, L. F. A. Azevedo, and I. B. de Paula

Citation: Physics of Fluids **29**, 062106 (2017); doi: 10.1063/1.4985717
View online: http://dx.doi.org/10.1063/1.4985717
View Table of Contents: http://aip.scitation.org/toc/phf/29/6
Published by the American Institute of Physics

Characterization of linear interfacial waves in a turbulent gas-liquid pipe flow

A. A. Ayati,[1] P. S. C. Farias,[2] L. F. A. Azevedo,[2] and I. B. de Paula[2]
[1]*Department of Mathematics, University of Oslo, N-0316 Oslo, Norway*
[2]*Departamento de Engenharia Mecânica, Pontifícia Universidade Católica do Rio de Janeiro - PUC-Rio, Rio de Janeiro, Brazil*

(Received 22 February 2017; accepted 31 May 2017; published online 21 June 2017)

The evolution of interfacial waves on a stratified flow was investigated experimentally for air-water flow in a horizontal pipe. Waves were introduced in the liquid level of stratified flow near the pipe entrance using an oscillating plate. The mean height of liquid layer and the fluctuations superimposed on this mean level were captured using high speed cameras. Digital image processing techniques were used to detect instantaneous interfaces along the pipe. The driving signal of the oscillating plate was controlled by a D/A board that was synchronized with acquisitions. This enabled to perform phase-locked acquisitions and to use ensemble average procedures. Thereby, it was possible to measure the temporal and spatial evolution of the disturbances introduced in the flow. In addition, phase-locked measurements of the velocity field in the liquid layer were performed using standard planar Particle Image Velocimetry (PIV). The velocity fields were extracted at a fixed streamwise location, whereas the measurements of the liquid level were performed at several locations along the pipe. The assessment of the setup was important for validation of the methodology proposed in this work, since it aimed at providing results for further comparisons with theoretical models and numerical simulations. Therefore, the work focuses on validation and characterization of interfacial waves within the linear regime. Results show that under controlled conditions, the wave development can be well captured and reproduced. In addition, linear waves were observed for liquid level oscillations lower than about 1.5% of the pipe diameter. It was not possible to accurately define an amplitude threshold for the appearance of nonlinear effects because it strongly depended on the wave frequency. According to the experimental findings, longer waves display characteristics similar to linear waves, while short ones exhibit a more complex evolution, even for low amplitudes. *Published by AIP Publishing.* [http://dx.doi.org/10.1063/1.4985717]

I. INTRODUCTION

The transport of gas and liquid simultaneously in horizontal pipelines is present in many engineering applications. During the last decades, an intense effort has been devoted to the study and modeling of the flow characteristics in order to increase safety and profit margins in pipeline operations, see Havre *et al.* (2000) for a review.

An important characteristic of two phase flows is the existence of a variety of flow regimes, depending on, among other variables, the flow rates of each phase. These regimes are defined based on the geometrical distribution of phases in the pipe cross section, see Mandhane *et al.* (1974) and Taitel and Dukler (1976). The present work is devoted to investigating horizontal stratified flows at conditions close to transition to intermittent flows.

According to Kordyban and Ranov (1970), the intermittent flow in horizontal pipes can be generated from the stratified flow by hydrodynamic instabilities, which promotes the growth of small perturbations present in the liquid interface. They derived a criterion for transition based on inviscid linear stability analysis, and discrepancies with the experimental results of Wallis and Dodson (1973) were observed. Later, Lin and Hanratty (1986), Barnea and Taitel (1989), and Barnea and Taitel (1993) extended the linear stability analysis to include viscous effects and derived a theoretical expression that showed reasonable agreement with reported low-pressure, small-scale data for low and medium gas flow rates. According to Bendiksen and Espedal (1992) and Kadri *et al.* (2009), for pipes with large diameters and high flow rates, there is still a discrepancy between the experimental findings and the theoretical predictions.

Andreussi *et al.* (1985) showed that non-linear roll-waves are possible solutions of the one-dimensional mass and momentum equations for gas and liquid. They suggested that the appearance of roll-waves could be related to slug initiation. Later, Soleimani and Hanratty (2003) used viscous long wavelength theory to predict the initiation of roll-waves and consequently the slug onset. Many other subsequent works have been devoted to investigate and to model slug initiation (Ansari and Shokri, 2011; Barmak *et al.*, 2016; Fan *et al.*, 1993; Funada and Joseph, 2001; Ujang *et al.*, 2006; and Valluri *et al.*, 2008). Although many aspects of the problem are included in the models, they are still not capable of predicting accurately the slug onset for a wide range of pipe diameters and flow rates. Some authors, such as Bontozoglou (1991), claim that non-linear effects, which are not included in most models, can play a crucial role in the transition process. More

recently, Sanchis *et al.* (2011) suggested that nonlinear wave-wave interactions can induce rapid growth of fluctuations in the liquid level and initiate slugs.

A remarkable progress of numerical tools for the simulation of two phase flows has been experienced in the last decades (Issa and Kempf, 2003). Some of these simulation tools are capable of predicting terrain generated slugs, but they often fail in predicting the formation of hydrodynamic slugs. For instance, in Sanchis *et al.* (2011), it is mentioned that some commercial numerical simulation tools widely used in industry, such as OLGA®, are not capable of predicting the formation of hydrodynamic slugs with reasonable accuracy.

Due to the complexity of the problem, it is, indeed, very difficult to establish a unique model which can be used for a wide range of flow parameters. A common procedure used for validation of both theoretical and numerical models is to correlate the onset of instability with the experimental data of slugs [see Sanchis *et al.* (2011) for a review]. To this end, statistical data about superficial velocities at which slugs first appear and slug shedding frequencies have been extensively used. For instance, the works Barnea and Taitel (1989), Barnea and Taitel (1993), Funada and Joseph (2001), and Kadri *et al.* (2009) compare predictions from linear stability models with measured slug statistics. Although shear rates related to phase velocities can influence the growth of disturbances via linear instability mechanisms, it is rather unclear whether these mechanisms are solely responsible for slug initiation. For a straightforward validation of models and simulations, it would be more convenient to have an experimental database about the development of interfacial waves, since most of the models are derived from the modal stability analysis of well-defined base flows. Andritsos and Hanratty (1987), Ayati *et al.* (2014; 2015; 2016), Birvalski *et al.* (2014), and Tzotzi and Andritsos (2013) address the problem of waves in stratified flows. Although many characteristics of the phenomenon are detailed in those works, no information about modal disturbances is found. Typically, for modal analysis, a controlled experiment is required [see Schmid and Henningson (2001) for a review]. However, the setup required to introduce disturbances with characteristics approaching that of most unstable eigenmodes, according to the stability analysis, is not found in the literature. Jurman *et al.* (1992) analyze experimentally the evolution and the interaction between interfacial waves in a rectangular channel for a rich spectrum of interfacial disturbances. However, no detailed information is found for single modes. For pipe flows, the number of studies is rather scarce and no similar study is found. Thus, there is an evident lack of experimental data for validation of recent models based on modal linear stability analysis like those given by Kaffel and Riaz (2015) and Barmak *et al.* (2016).

In view of the current state of affairs, it appeared that further work in a regime of controlled waves on a stratified gas-liquid flow would be of interest. In the present work, disturbances are introduced near the pipe entrance and their subsequent evolution is measured for different mixture velocities. The focus is on linear stages of wave development; therefore, only waves with small amplitudes are examined.

This manuscript is organized as follows: After this introduction, the experimental setup and methodology are described. Thereafter, the selection of experimental parameters for the linear regime of wave evolution is addressed. The main results are then presented in the form of a characterization of waves within the linear regime. In Sec. IV, main conclusions from the work are summarized and discussed.

II. EXPERIMENTAL SETUP

A schematic view of the test rig used in the experiment is presented in Fig. 1. The pipeline was fabricated from Fluorinated Ethylene Propylene (FEP) with an internal diameter (D) of 0.0508 m and length (L) of 8 m, yielding a 150 diameter long tube. The FEP material has nearly the same refractive index as water providing reduced light scattering and allowing

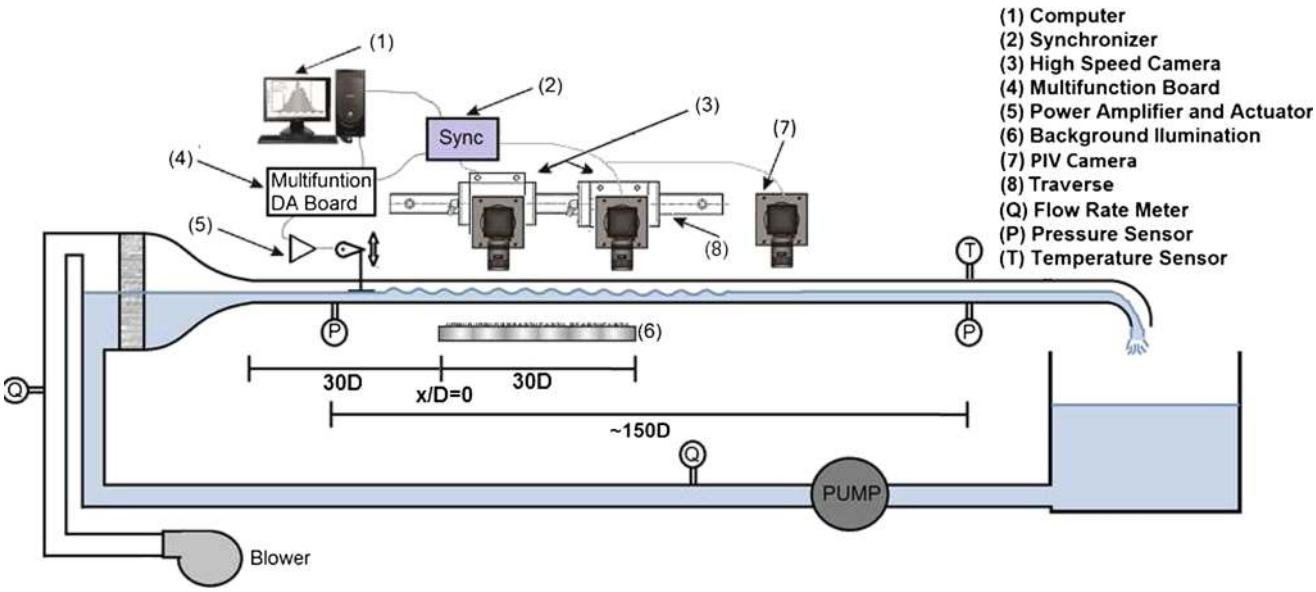

FIG. 1. Schematic view of the experimental setup used in this study.

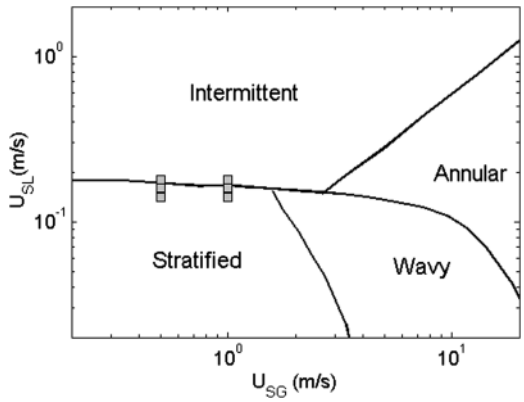

FIG. 2. Flow regime map. Symbols indicate experimental conditions selected for this investigation. Base map extracted from the work of Mandhane *et al.* (1974).

the liquid film visualization at regions very close to the pipe wall (Hewitt *et al.*, 1990).

Air was supplied to the test section by a centrifugal compressor which can reach velocities up to 40 m/s. Superficial liquid velocities up to 0.5 m/s were provided by a progressive cavity pump. Air and water flow rates were measured using the calibrated turbines, CONTECH® models SVTG G19 and SVTL L19, with experimental uncertainties estimated to be within 1% and 0.5%, respectively. Current investigations were performed for liquid and gas velocities within the range of [0.16; 0.18] m/s and [0.5; 1.0] m/s, respectively. The corresponding Reynolds numbers based on superficial liquid and gas velocities were [8128; 9144] and [16 933; 33 867].

It is didactically important to display the conditions selected for this investigation in a map of flow regimes, as illustrated in Fig. 2. The reference map in the figure was extracted from the work of Mandhane *et al.* (1974). The geometry and the fluids adopted in that work are similar to those of current investigation. According to the figure, the range studied here covers the transition from smooth stratified to intermittent flow regimes. At such flow rates, disturbances are close to a neutrally stable condition, yielding weak damping/amplification rates. Thereby, the evolution of disturbances is expected to display a slow variation with the axial coordinate, hence facilitating its measurement along the pipeline.

Air and water were injected by a special mixer which was designed using concepts employed in low turbulence water tunnel facilities (Wetzel and Arndt, 1994). The mixer was located at the inlet section of the tube. Flow conditioners were introduced downstream of the settling chamber in order to remove swirl and fluctuations of high amplitudes. Further downstream, a contraction with the cubic shape, designed according to Wetzel and Arndt (1994), provided a smooth acceleration of both fluids toward the pipe inlet. At the end of the line, the air-water mixture was directed towards a high volume separator vessel in which fluctuations were damped. The water returned to the pump inlet, while the air was vented out of the laboratory space.

Controlled disturbances were generated at the liquid-gas interface near the pipe entrance using an oscillating plate. Relatively low energy is required to excite disturbances at the interface, implying a limited range of movement for the plate. Thereby, the disturbances are introduced mainly on the liquid level and not in the components of the base flow velocities.

A multifunction D/A board NI AT-MIO-16X was used to control the movement of the oscillating plate. This setup is capable of generating arbitrary waveforms. A power amplifier with unity gain was used to drive the actuator that consists of a head positioning system of a common hard disk drive. The axis of rotation of the actuator was coupled to the knob of a radial potentiometer to monitor, in real time, the movement of the actuator and transform it into a displacement in mm. In the present work, the waves at frequencies of 4 and 6 Hz were generated by the controlled system implemented.

Images of the liquid film were captured using two IDT Motion Pro X3 high frame rate digital cameras with 1.3 MP resolution. The cameras were mounted approximately 20 pipe diameters downstream of the wave generation source. The cameras were mounted orthogonally to a high power white light emitting diode (LED) light panel, which provided sufficient background illumination for image acquisition. A BNC 575 synchronizer allowed the synchronization between the generation of disturbances and the image acquisition. An image processing algorithm was developed to automatically detect the position of the air-water interface in each image frame.

A. Image processing—shadow technique

A non-intrusive shadow technique, based on the work of Nogueira *et al.* (2003), was employed to provide time-resolved liquid height information. This technique relies on digital cameras to capture the intense and uniform background light that passes through the flow, as illustrated in Fig. 3. In the present study, the camera field of view was approximately 5*D*. The acquisition of longitudinal images was synchronized with the signal of the actuator, allowing us to

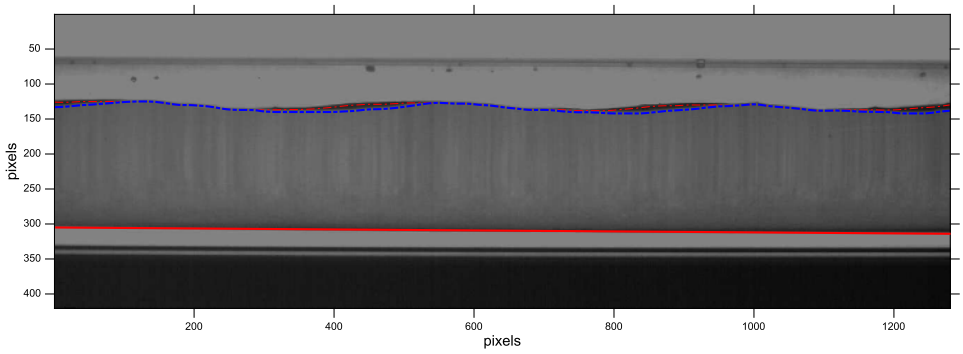

FIG. 3. Interface detected by binarization threshold (blue dashed-dotted) and distinction from back wall reflection (red dashed-dotted). The detected pipe bottom (red line) provided the reference level y = 0. Flow conditions: U_{SG} = 1.0 m/s and U_{SL} = 0.21 m/s.

perform phase-locked acquisitions, thus providing temporal and spatial evolution of the disturbances generated by the oscillating plate.

Instantaneous images were pre-processed with the objective of enhancing contrast through the intensity histogram smoothing and equalization procedure. This procedure not only removes any bias that could have been introduced by differences in illumination intensity, but also facilitates the determination of the binarization threshold for identifying liquid-gas interface contours, see Gonzales *et al.* (2009) for a review of the standard image processing routines.

A small amount of blue dye was added to water in order to enhance the intensity contrast. At the interface between the two fluids, the passage of light was attenuated, creating a shadow on the acquired image. Due to the pipe curvature, a shadow stemming from the interface intersection with the back wall of the pipe, closest to the light source, was shed on to the image. Hence, the image often consisted of two possible edges to represent the interface. The upper edge originated from the back wall intersection, while the lower edge stemmed from the front wall intersection. In this study, it is the foremost interface/wall intersection that is taken as the interface position of interest. In Fig. 3, a dashed-dotted blue line corresponding to the measured film height is overlaid on the original image in order to illustrate the accuracy of the interface detection. A calibration operation was necessary to convert from pixels to real dimensions. The edges of the pipe were used as a reference. Before every set of measurements, the calibrations were checked.

The synchronization between acquisition and disturbance generation is demonstrated in Fig. 4. The figure shows a set of contours obtained from 60 different images captured at a distance of 15D from the disturbance source. An excellent agreement was found showing that, indeed, excited waves were phase-locked with respect to data acquisitions. Some degree of scattering was observed, but this could be considered as normal because both phases were turbulent and hence non-controlled disturbances were always present in the flow.

The frequency content of the paddle oscillation is analyzed in the spectra of Figs. 5(a) and 5(b), in order to assess whether generated waves were composed by a single Fourier mode. This is important since the focus of this study is the characterization of waves within the linear regime; therefore, excitation of multiple waves must be avoided. The spectra of Figs. 5(a) and 5(b) display a sharp peak around the excited

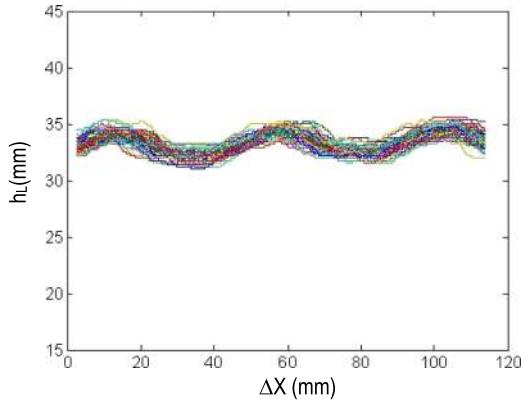

FIG. 4. Example of interface detection from 60 different images. Flow conditions: U_{SG} = 1.0 m/s and U_{SL} = 0.21 m/s.

frequencies, indicating that disturbances were, indeed, mostly introduced at the selected frequencies. Small amount (less than 15%) of energy contamination to harmonic components was observed.

B. Assessment of methodology

In view of the high sensitivity of wave development to the flow conditions, a series of preliminary tests were performed in order to assess the quality of the results obtained with the test rig. This is an important part of the experiment because the results must be reproducible for further comparisons with simulations and theoretical models.

One of the most influential parameters in the development of interfacial waves is the mean liquid level. Thus, it is important to maintain this parameter constant during measurements. However, this can be quite challenging when operating at conditions close to transition to slug flows. Depending on the liquid and gas flow rates, waves could grow and initiate slugs further downstream from the excitation location. Such slugs are capable of capturing a high amount of liquid as they propagate along the pipe. This changes the flow conditions, including the mean liquid level, both upstream and downstream of the point of slug initiation.

In order to avoid the influence of slugs on the results, disturbances were introduced in the flow as wave trains and not as continuous waves. Since slugs can significantly affect the flow at stations upstream its initiation, the procedure is adopted to ensure that no data are acquired when slugs are present in the

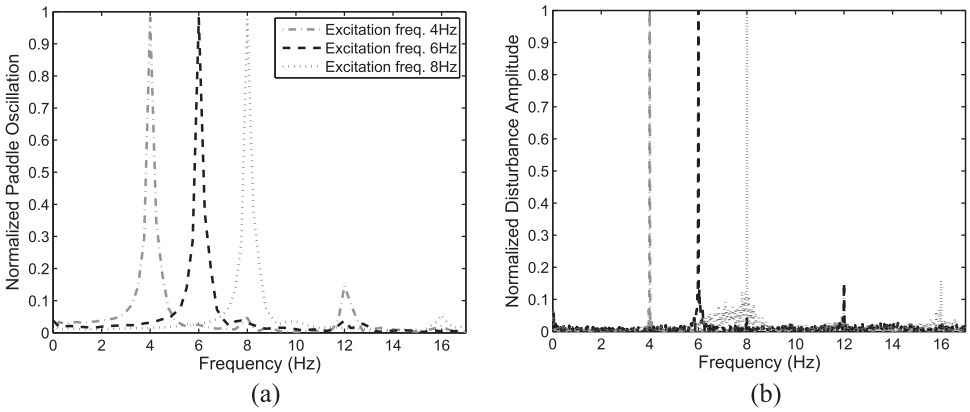

FIG. 5. Normalized Fourier spectra of excited disturbances for three different driving frequencies, namely, 4 Hz, 6 Hz, and 8 Hz. Flow conditions: U_{SG} = 1.0 m/s and U_{SL} = 0.21 m/s. (a) Spectra of paddle oscillation. (b) Initial interface oscillation.

pipeline. Image acquisitions were synchronized with the central part of the wave train, where the waves displayed constant amplitude and spectral content. Blocks of only 20 images were collected per wave train at a constant frame rate of 40 Hz. Thereby, the acquired images would appear as a continuous movie if displayed in a sequence. The time elapsed between consecutive wave trains had to be long enough to enable a complete recovery of the base flow conditions. Preliminary tests have shown that 40 s after the slug initiation the base flow was completely recovered. For cases with no slug initiation, long lasting wave trains were introduced and blocks of 2000 images per camera position were acquired continuously.

Prior to the measurements, it was necessary to define the minimum number of blocks required for the convergence of wave statistics. For this test, a challenging measurement condition was selected. This corresponded to a regime with slug initiation close to the pipe outlet. At every repetition, a block containing 20 images was acquired. This test was important to observe whether variations in flow conditions during the tests would avoid convergence of the results. Mean liquid height and FFT amplitudes were analyzed for an increasing number of acquired blocks. The results are presented in Fig. 6. For this test, the liquid and gas velocities were set to 0.21 m/s and 1 m/s, respectively, and the excitation frequency was set to 4 Hz.

The statistics were evaluated with cameras positioned at the furthest position possible away from the perturbation site. The figures suggest a substantial variation of wave statistics for less than 50 repetitions. A satisfying convergence of data is seen when more than 80 blocks were considered. All subsequent measurements were conducted with the slightly conservative number of 100 blocks, which corresponded to 2000 images per camera position.

It was also necessary to verify the reproducibility of amplification curves for different ambient conditions. This was tested by comparing experiments performed in different days. The results of the evolution of the waves are presented in Fig. 7 for three different runs under fixed gas and liquid superficial velocities of 1 m/s and 0.16 m/s, respectively. The figure illustrates that all three amplification curves display

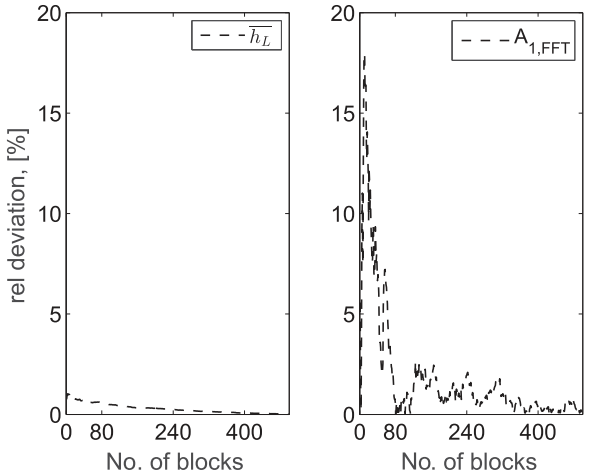

FIG. 6. Convergence of A_{FFT} and $\overline{h_L}$. Flow conditions: U_{SG} = 1.0 m/s and U_{SL} = 0.21 m/s.

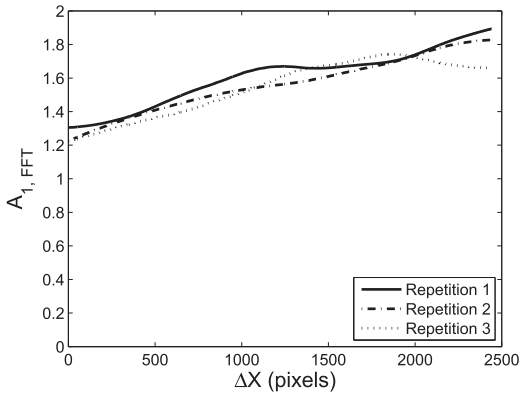

FIG. 7. Example of reproducibility. Measurements of wave height evolution performed at fixed frequency and flow rates in different days. Flow conditions: U_{SG} = 1.0 m/s and U_{SL} = 0.16 m/s.

similar behavior, thus demonstrating that the experiment is reproducible to a satisfactory degree.

C. Analysis of velocity fields in the liquid layer—PIV technique

Velocity fields in the liquid layer were measured with a planar PIV setup, which consisted of one TSI Powerplus 4 MP camera with resolution 2048 × 2048 pixels and a double-pulse Nd:YAG laser capable of delivering 200 mJ/laser pulse. Due to optical alignment, the camera and the laser optics were placed at a fixed position. Thus, the velocity fields were obtained for a single streamwise location corresponding to 100D from the pipe inlet.

Furthermore, the test section was equipped with a rectangular optical box filled with water, matching the refracting index of the FEP pipe, hence reducing distortion caused by the pipe wall. The water was seeded with spherical polyamide particles with an average diameter $\bar{d} \sim 50\ \mu$m and with nearly zero buoyancy.

Sets of 1000 image pairs were acquired with a sampling rate of 5 Hz, that being the maximum rate of acquisition allowed by the camera in use. The total field of view was set to 1.4D × 1D. Note that in this figure, the y-axis is normalized with the interfacial position, y_i. The interrogation process of the recorded PIV realizations was carried out with TSI's commercial software, Insight 4G, using 64 × 64 pixels interrogation windows and 50% overlap. Hence, the final sub-window size was 32 × 32 pixels, resulting in 63 displacement vectors in each spatial direction (x and y).

The acquisition was synchronized with the disturbance source. Thereby, ensemble average techniques could be employed. The periodicity of the waves within the series of acquired images allowed us to resolve the excited disturbances exactly at the disturbance frequency. Thus, the standard fast Fourier transform algorithms were used for data analysis. However, due to the limited sampling frequency of the camera, i.e., lower than the Nyquist frequency, relevant fluctuations appeared as the aliased signal in the Fourier domain. Nevertheless, the frequency of the aliased signal could be easily retrieved using the following equation:

$$f_a = |nF_s - f_s|. \tag{1}$$

Here, f_a is the aliased frequency of the sampled signal f_s, while F_s is the sampling frequency and n is the closest integer multiple of the sampling frequency to the signal being aliased.

III. LINEAR REGIME OF WAVE EVOLUTION

The linear approach for any system is typically restricted by the amplitude of the disturbances. Unfortunately, the authors were not able to find a ubiquitous amplitude threshold to define a linear range for the evolution of interfacial waves in a stratified gas-liquid pipe flow in the literature. Thus, prior to the characterization of interfacial waves, a set of preliminary experiments were performed to ensure that excited disturbances were within the linear regime in the measurement domain.

A. Experimental determination of linear wave regime

At first, it was necessary to define an amplitude threshold for waves to be considered as linear. For this test, the driving voltage of the oscillating paddle was varied and the resulting change in amplitude of interfacial waves was monitored at the farthest measurement station downstream from the paddle ($\approx x/D = 30$). The idea is to find a range of wave amplitudes where a linear scaling is observed between excitations and waves measured at the last streamwise station. A similar procedure was previously used in the work of de Paula *et al.* (2013) to describe linear stages of instability waves in boundary layers. Here, the waves at frequencies of 4 and 6 Hz were analyzed. It is relevant to mention that the waves excited at frequencies higher than 6 Hz were also measured, but their behavior was more complex and a linear regime of evolution was not clearly identified. The analysis of these waves demands a different approach from the one proposed here, and a description of two different methodologies would excessively extend the manuscript. Thus, nonlinear evolution of interfacial waves is intended to be addressed further in a continuation of the current study.

According to the results of Figs. 8(a) and 8(b), no evident amplitude threshold was observed. However, waves having amplitudes below $0.015D$ seem to scale linearly with the excitations for all cases shown in the figure. Apparently, this is a conservative threshold, but it was assumed as an amplitude limit for the present work in order to avoid the influence of nonlinear effects on the experimental results.

The spectral evolution of interfacial waves having amplitudes lower than the threshold defined in the first set of tests was analyzed for different gas and liquid velocities. Results are depicted in Figs. 9 and 10, for excitation frequencies of 4 and 6 Hz, respectively. The amplitudes in the spectra are normalized by the excited wave amplitude at the first measurement location, namely, $X = 0D$. Although the spectral information is available at a much higher resolution, only discrete stations are shown in Figs. 9 and 10. All these features facilitate a direct comparison of the results obtained for different test conditions.

The spectra of Fig. 9 show no evidence of any strong influence from subharmonics or harmonics of the excited wave on oscillations at the liquid interface. The results are somehow

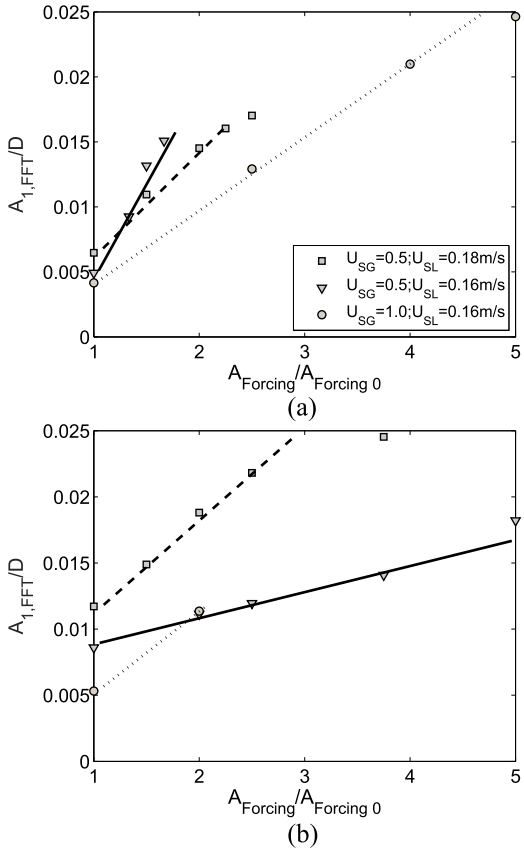

FIG. 8. Variation of wave amplitude at the last measurement station according to the forcing amplitude. (a) 4 Hz and (b) 6 Hz.

similar to those reported in the work of Bar-Cohen *et al.* (2016) for interfacial waves in microchannels. In that work, waves did not exhibit substantial variation of wavelength even after entering the non-linear wave regime. In Figs. 9(a) and 9(b), which correspond to cases with a fixed superficial gas velocity of 0.5 m/s, harmonics having low amplitudes could be found at initial stations. Further downstream such high frequencies decay, or simply do not grow as the waves develop. The level of noise in the spectra of Fig. 9(d) is higher in comparison to other cases. This might be linked to the instability of base flow, since this case is closer to the transition from a smooth stratified to a wavy flow regime.

For waves excited with a frequency of 6 Hz, the presence of harmonics is more evident as shown in the spectra of Fig. 10. Nevertheless, the amplitude of the harmonics was significantly smaller in comparison to the excited disturbances. Overall, the spectra presented in Fig. 10 display qualitatively the same behavior as those from Fig. 9. Thus, it can be stated that no evidence of strong wave-wave interactions could be found in these preliminary experiments.

It is well known from hydrodynamic instability studies that nonlinear disturbances can affect the base flow, see Schmid *et al.* (2002) for a review. In a linear regime, such an effect is not observed and the base flow is not modified when disturbances are present. In order to assess whether the waves investigated were, indeed, within the linear regime, the mean liquid height was monitored for different forcing amplitudes. Results are depicted in Fig. 11. Measurements performed for different wave frequencies are combined in the same plot. According

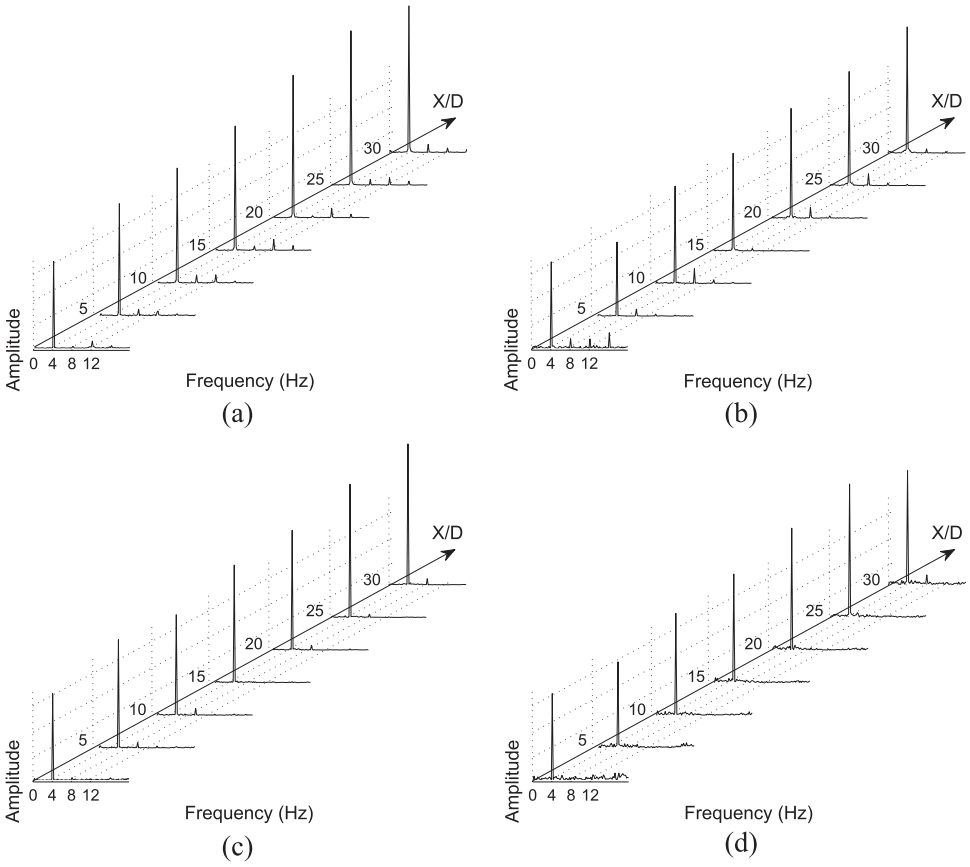

FIG. 9. Spectral evolution of interfacial disturbances for different superficial liquid and gas velocities. Excitation frequency, 4 Hz. (a) U_{sg} = 0.50 m/s, U_{sl} = 0.16 m/s. (b) U_{sg} = 0.50 m/s, U_{sl} = 0.18 m/s. (c) U_{sg} = 1.00 m/s, U_{sl} = 0.16 m/s. (d) U_{sg} = 1.00 m/s, U_{sl} = 0.18 m/s.

to the results, a small decrement in the mean liquid height was observed for wave amplitudes higher than 0.015D. Amplitudes smaller than 0.015D induced no change in mean liquid height. This is in line with the amplitude threshold defined in the linearity test of Fig. 8. The current findings strongly suggest that interfacial waves with amplitudes smaller than 0.015D are

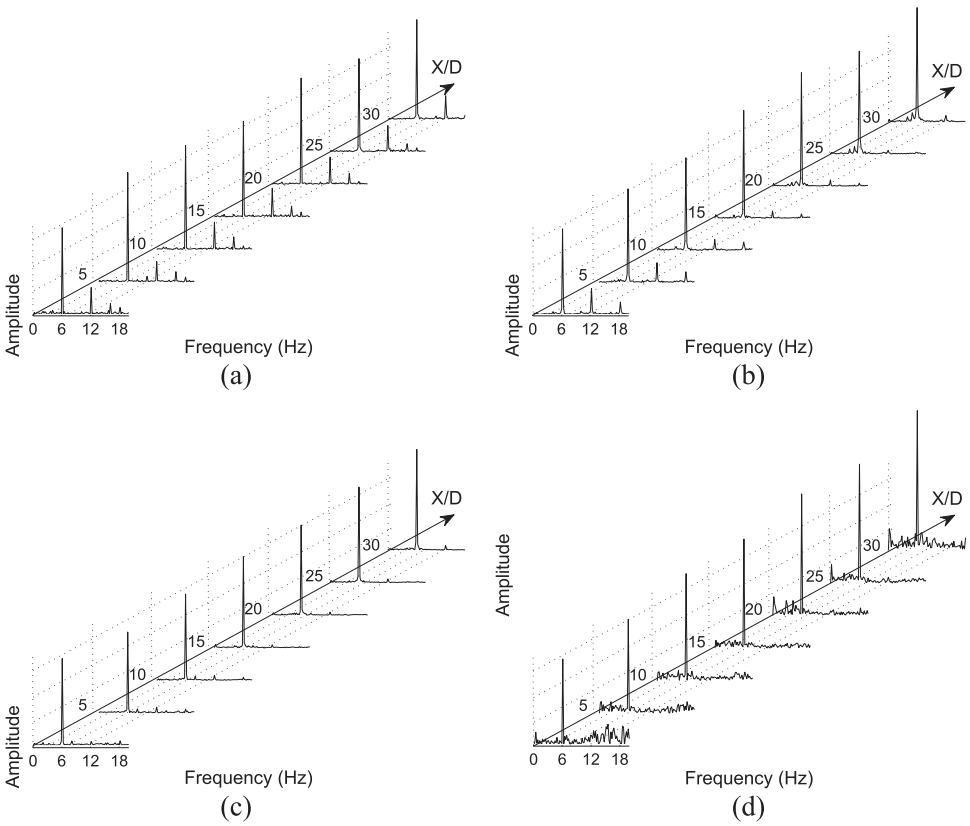

FIG. 10. Spectral evolution of interfacial disturbances for different superficial liquid and gas velocities. Excitation frequency, 6 Hz. (a) U_{sg} = 0.50 m/s, U_{sl} = 0.16 m/s. (b) U_{sg} = 0.50 m/s, U_{sl} = 0.18 m/s. (c) U_{sg} = 1.00 m/s, U_{sl} = 0.16 m/s. (d) U_{sg} = 1.00 m/s, U_{sl} = 0.18 m/s.

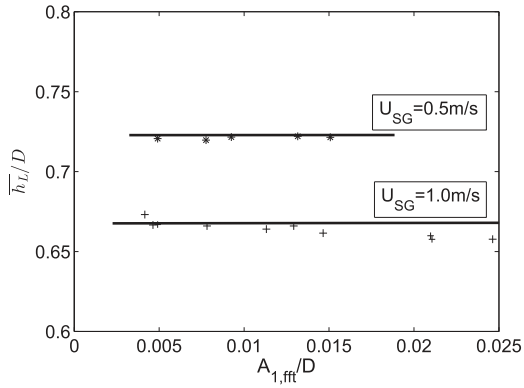

FIG. 11. Variation of mean liquid height with the wave amplitude for U_{SL} = 0.16 m/s.

linear within the flow rates analyzed. Thus, the characteristics of these waves are detailed in Sec. III B.

B. Characterization of waves

According to Kaffel and Riaz (2015), detailed characterization of the interfacial waves has been carried out mostly for two-phase boundary layer and shear flow problems. Channel and pipe flows are rather less explored. Up to date, most of theoretical works address the problem when both phases are laminar. Indeed, turbulent two-phase flow modeling is challenging due to the interactions between the turbulence and the interface which can be coupled and lead to a modification of the flow. Recently, Ayati *et al.* (2015) used PIV measurements to observe the interaction between turbulence in the gas and interfacial waves. In the reported scenario, accurate stability predictions are rather difficult because turbulence can actively modify the wave development. An experimental characterization of interfacial waves is important for validation of models. Here, some features of small amplitude interfacial waves were measured using shadowgraphy and phase-locked acquisitions. Characteristics such as wavenumber, celerity, and wave growth are obtained and reported. Similar data for waves composed by a single Fourier mode were not found in the literature. The results can shed some additional light on how the two-phase boundary layer problem compares with the two-phase channel and pipe flows.

The measured phase evolution of the waves is shown in Figs. 12(a) and 12(b). Phases were extracted from the spectra of interfacial oscillations. The spatial resolution of the measurement was rather high, i.e., one time series per camera pixel. In order to avoid excessive amount of data in the graph, only phases from every 120 pixel are shown. It is worth to mention that no averaging or smoothing was applied to the data. Only phase corrections of 2π and its multiples were employed to account for complete wave cycles. The results show a linear phase variation of the waves for almost the whole measurement region. The only exception was the case with a wave frequency of 6 Hz at the highest mixture velocity. In this case, there was a phase variation close to the end of the measurement region. This is apparently linked to the initial stages of nonlinear wave evolution. A detailed analysis of these stages is out of scope from this work, but the topic should be addressed in future works.

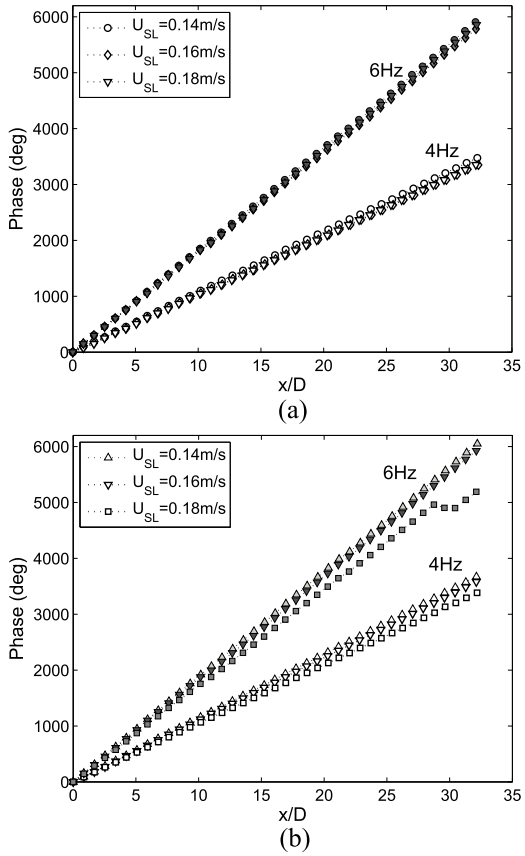

FIG. 12. Phase evolution of waves for different superficial velocities and wave frequencies. Open and filled symbols correspond to waves with frequencies of 4 Hz and 6 Hz, respectively. (a) U_{SG} = 0.5 m/s. (b) U_{SG} = 1.0.m/s.

According to Fig. 12, phase increment of the waves was slightly modified by liquid and gas velocities. For increasing liquid velocity, it was expected to observe longer wavelengths. This tendency is qualitatively confirmed in the plots. On the other hand, higher superficial gas velocities induced a small shortening of the waves. Wave numbers were obtained from the phase evolution curves using linear curve fit. The same information could also be obtained using auto-correlation of the liquid film interface. However, this procedure was more expensive and less accurate than curve fitting. A compilation of the information extracted from these measurements is given

TABLE I. Wave properties and mean liquid height for different flow rates and wave frequencies.

U_{SL} (m/s)	U_{SG} (m/s)	F (Hz)	k (m^{-1})	c (m/s)	$\overline{h_L}/D$
0.14	0.5	4	6.0	0.67	0.704
0.16	0.5	4	5.8	0.69	0.726
0.18	0.5	4	5.8	0.69	0.768
0.14	1.0	4	6.4	0.63	0.647
0.16	1.0	4	6.2	0.65	0.660
0.18	1.0	4	5.9	0.68	0.705
0.14	0.5	6	10.2	0.59	0.695
0.16	0.5	6	10.0	0.6	0.729
0.18	0.5	6	10.1	0.59	0.771
0.14	1.0	6	10.4	0.58	0.657
0.16	1.0	6	10.2	0.59	0.663
0.18	1.0	6	9.6	0.63	0.709

TABLE II. Wave celerity given by different linear models.

Linear theory	Wave celerity
Shallow water	$c_{sw} = \sqrt{gh_L}$
Finite depth	$c_{fd} = \sqrt{\frac{g}{k}\tanh(kh_L)}$
Capillary-gravity	$c_{cg} = \sqrt{\left(\frac{g}{k} + \frac{\sigma}{\rho}k\right)\tanh(kh_L)}$
Interfacial waves	$c_{iw} = \sqrt{\frac{g(\rho_L - \rho_G)}{k(\rho_L \coth(kh_L) + \rho_G \coth(kh_G))}}$

in Table I. It also includes the mean level of liquid in the pipe.

The measured wave celerity was compared with different linear wave dispersion relations. Johnson *et al.* (2009) and Sanchis *et al.* (2011) observed that the dominant phase velocity of interfacial waves propagating on a thin liquid layer can be matched with linear shallow water wave theory. However, shallow water wave theory is valid only when the wavelength is much smaller than the water depth and this condition is not necessarily satisfied in the current experiment. Thus, the measured celerity was compared with other classical dispersion relations derived for linear waves at a finite depth. A list of dispersion relations used in this comparison are given in Table II [for reference, see Landau and Lifshitz (1987)]. In order to account for the Doppler-shift introduced by the mean flow, the liquid velocity was subtracted from the measured wave velocities.

According to Fig. 13, theories based on finite depth are in better agreement with the experimental findings. Furthermore, corrections introduced by different finite depth theories are not significant. Thus, within the range of parameters analyzed, there was no evident contribution from the surface tension and gas density to the wave celerity. The only dispersion relation in complete disagreement with the experiments was the shallow water equation. Although the experiments are only in qualitative agreement with the other theories, the results strongly suggest that the shallow water relation is not appropriate to model interfacial waves in pipe flows. Similar observations are reported in the work of Ayati *et al.* (2014) for wavy flows.

The amplitude growth of interfacial waves was also observed for different test conditions. Results obtained for disturbances with a frequency of 4 Hz are depicted in Figs. 14(a) and 14(b). Similar to the phase analysis, only points at every 120 pixels are shown in the figure. Curves were normalized by amplitudes at the first measurement station (x/D = 0). Amplitude growth predicted by a linear, 1-D viscous Kelvin-Helmholtz model, as proposed in the work of Barnea and Taitel (1993), was also included in the figure for a comparative analysis. Temporal growth rates predicted by that model were converted into spatial ones using Gaster's transformation [see Schmid *et al.* (2002) for a review]. According to these figures, amplification is stronger for increasingly higher liquid flow rates. Apparently, variations in the gas flow rate had minor influence on the wave growth. This is consistent with the picture drawn from flow regime maps, such as those from the works of Barnea (1987), Mandhane *et al.* (1974), Taitel and Dukler (1976), and many others. In general, those maps point towards higher influence of the liquid velocity on the stability of smooth stratified flow. This is, however, valid only for gas velocities remarkably lower than the transition limit to wavy or to annular flow regimes. Indeed, this is the condition of present experiments.

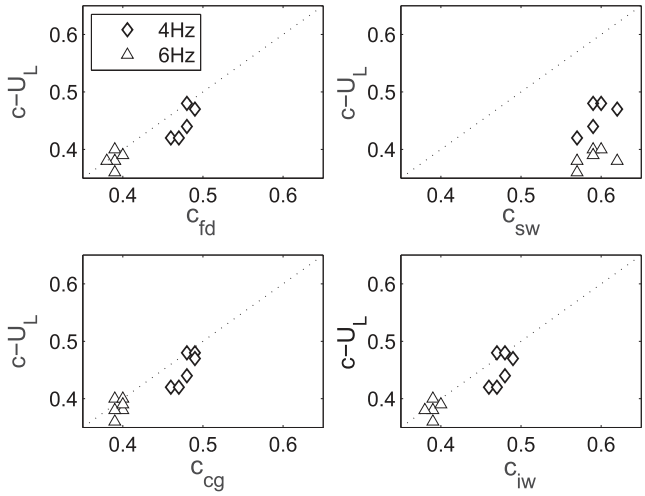

FIG. 13. Wave celerity.

The curves in Figs. 14(a) and 14(b) show linear amplification in a log scale. To the authors' knowledge, this is the first time that such a behavior is captured experimentally for a gas-liquid pipe flow. No evidence of other mechanisms than the instability of the interfacial waves was observed within the streamwise domain analyzed. For a linear regime, results suggest that wind shearing effects and gas turbulence are not strong enough to influence the growth of waves with a frequency of 4 Hz. In addition, curves related to the Viscous

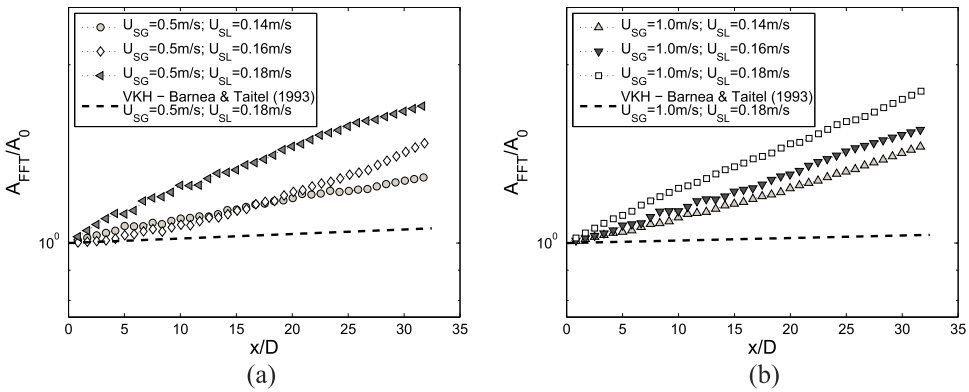

FIG. 14. Wave growth along the pipe axis for three different flow rate combinations. Perturbation frequency, 4 Hz. (a) U_{sg} = 0.50 m/s. (b) U_{sg} = 1 m/s.

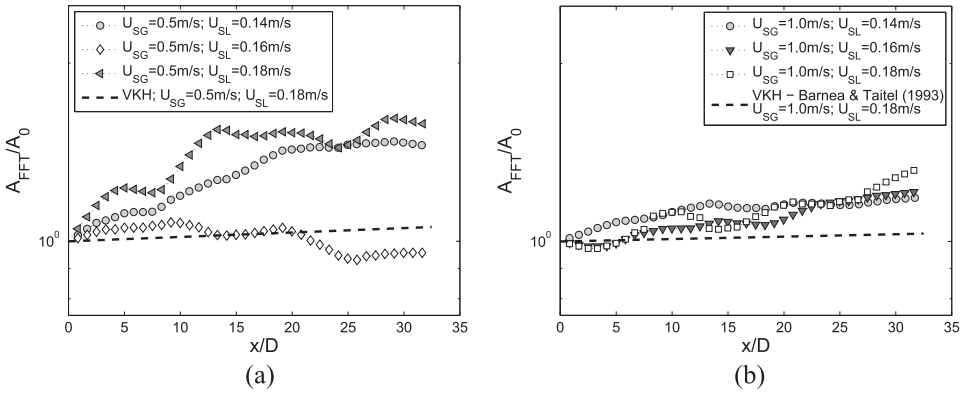

FIG. 15. Wave growth along the pipe axis for three different flow rate combinations. Perturbation frequency, 6 Hz. (a) U_{sg} = 0.50 m/s. (b) U_{sg} = 1 m/s.

Kelvin-Helmholtz (VKH) model proposed in the work of Barnea and Taitel (1993) displayed a significant deviation from the measurements. There are several possible reasons for these discrepancies. Further work is necessary to investigate whether simple 1-D models can be properly tuned for a reasonable estimation of wave growth in turbulent flows. However, this is out of scope of present work and is therefore not addressed here.

Amplitude evolution of waves excited with a higher frequency of 6 Hz does not exhibit a monotonic growth as illustrated in Figs. 15(a) and 15(b). According to Fig. 15(a), no coherent tendency of amplification or decay was identified for different flow rates. Although in some cases the waves did apparently grow, the amplification exhibited was far from a linear trend. In Fig. 15(b), the amplitude oscillation along the pipe was less pronounced, but again no tendency was observed. The result is quite interesting because it shows that small variation in the wavelength scale could substantially modify the dynamic of the waves. Due to the constant phase increment observed in Figs. 12(a) and 12(b), this change in the wave dynamics might be related to weak nonlinear mechanisms. A weak nonlinear wave interaction, such as the one proposed by Sanchis *et al.* (2011), might not explain the current findings because here amplitudes of disturbances are very low. In the viewpoint of the authors, the influence of gas turbulence has more potential for destabilization of the interfacial waves with high frequencies and short wavelengths, i.e., higher steepness. The conjectured mechanism is somehow similar to the one observed by Buckley and Veron (2016) in a wind-wave-tank and by Ayati *et al.* (2015) in a pipe. In this case, boundary layer separation of gas flow at the wave crest can couple with the wave and cause the effect observed. However, the conjecture raised lacks of support and therefore it requires further investigations.

C. Base flow and eigenfunctions

In this section, the base flow and eigenfunction profiles of interfacial waves are measured in the liquid layer using planar PIV. The recent works of Kaffel and Riaz (2015) and Barmak *et al.* (2016) investigated the coalescence of shear and interfacial modes in a channel flow. According to Kaffel and Riaz (2015), eigenfunction profiles are not well investigated for channel flows. For pipe flows, the experimental evidence of eigenfunctions related to interfacial waves is nearly absent. Thus, eigenfunctions corresponding to interfacial instability modes were carefully measured in the liquid layer. Prior to measuring eigenfunctions, it is important to characterize the base flow and the turbulence intensity. The corresponding profiles for streamwise base flow velocity as well as streamwise and wall normal fluctuations are shown in Figs. 16(a)–16(c).

Profiles of mean flow velocity in Fig. 16(a) display a small increment in the velocity close to the interface. This is typical for liquid layers in smooth stratified flows, as observed previously in the works of Ayati *et al.* (2014) and Birvalski *et al.* (2014). According to Ayati *et al.* (2014) and Birvalski *et al.* (2014), base flow profiles of wavy flows typically exhibit a small velocity decrement close to the interface. This was not observed here, under low disturbance conditions.

Streamwise and wall normal velocity fluctuations, depicted in Figs. 16(b) and 16(c), respectively, do also show qualitative similarities with results reported in the literature for a smooth stratified flow (Ayati *et al.*, 2014 and Birvalski *et al.*, 2014). Profiles of streamwise velocity fluctuations display higher turbulence intensities near the wall and close to the interface. Apparently, the intensity peak close to the wall is related to wall shear disturbances of turbulent flows, whereas higher intensity at the interface is linked to interfacial disturbances. To date, it is not yet clear if these two disturbances are coupled in turbulent flows due to the high intensity of fluctuations close to the wall, which cannot be regarded as infinitesimal for linearization of the problem. Wall normal fluctuations illustrated in Fig. 16(c) display high intensities in the bulk of the liquid layer. Thus, no evident separation between the inner and interfacial disturbances could be extracted from this figure. In order to shed additional light on the physics of this problem, the inner disturbances and the interfacial ones were analyzed separately.

One of the main advantages of phase-locked measurements combined with controlled excitation of disturbances is the capability of extraction of coherent oscillations from the noisy signals. To this end, simple spectral decomposition is enough to enable extraction of coherent part of the signal. Thereby, portions of the turbulence intensity profiles related to the wave frequency were analyzed separately. These fluctuations corresponded to the eigenfunctions of the interfacial waves.

The eigenfunctions of streamwise and wall normal fluctuations are shown in Figs. 17(a) and 17(b) for waves with a

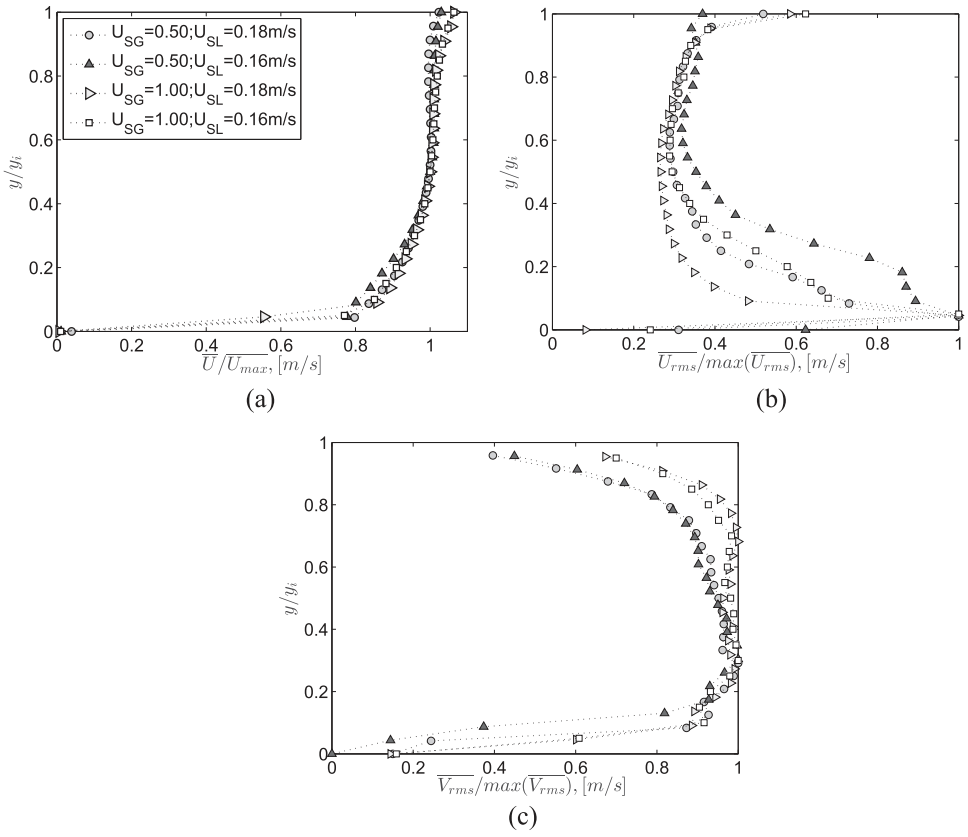

FIG. 16. Mean liquid velocity and RMS of fluctuations at a low disturbance condition, i.e., A_{rms}/D below 0.01. (a) Mean velocity. (b) U′ fluctuations. (c) V′ fluctuations.

frequency of 4 Hz. The waves reached amplitudes of around $0.025D$ at the measurement station due to the growth of disturbances along the pipe. Although amplitudes were higher than the threshold suggested in Fig. 8, the measured base flows were approximately similar to those shown in Fig. 16(a). Therefore, nonlinear effects would be weak, if they were present, and hence the measured eigenfunctions would closely represent those related to linear interfacial waves. In general, the shapes of the eigenfunctions of Fig. 17 were not modified for the tested conditions. The profiles of ϕ'_u display a peak at the interface, but their amplitude nearly vanishes at the bottom wall. The current findings support the explanation aforementioned on the nature of the two peaks in the profile of streamwise fluctuations. According to Fig. 17(a), the lower peak is, indeed, not related to the interfacial mode. In Fig. 17(b), the eigenfunction of ϕ'_v displays a peak slightly below the interface. The picture is qualitatively similar to the eigenfunctions found in the works of Kaffel and Riaz (2015) and Barmak *et al.* (2016).

In Figs. 18(a) and 18(b), waves with an oscillation frequency of 6 Hz show eigenfunctions, qualitatively, similar to those obtained for an excitation frequency of 4 Hz. However, in the case of Fig. 18, the profiles are rather noisy, possibly due to the low amplitude of the disturbances and to the interactions with turbulence. Interestingly, the near-wall peak in the streamwise fluctuation profile is more pronounced. This can be related to a lower signal to noise ratio. Thus, the contribution from near wall turbulence might not be completely removed from phase averaged signals. Another plausible argument is the coupling between interfacial waves and near wall disturbances via a mechanism analogue to that described in the work of Kaffel and Riaz (2015). However, this conjecture demands further investigation before any conclusion can be drawn.

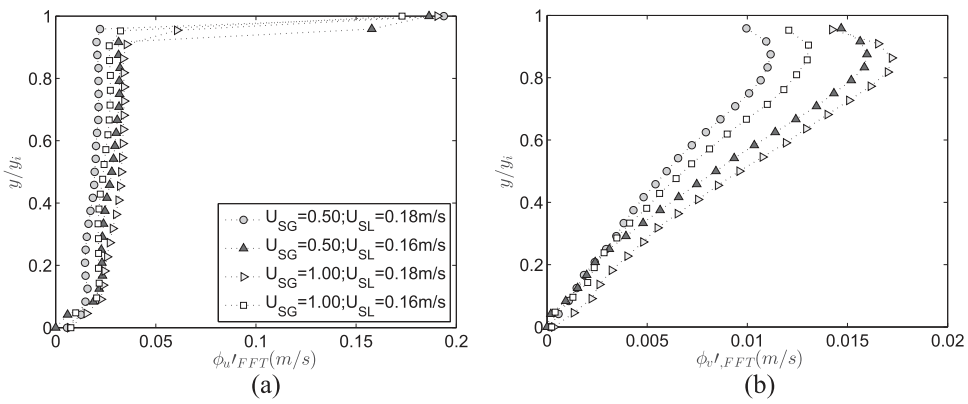

FIG. 17. Eigenfunctions of 4 Hz. (a) Streamwise. (b) Wall normal.

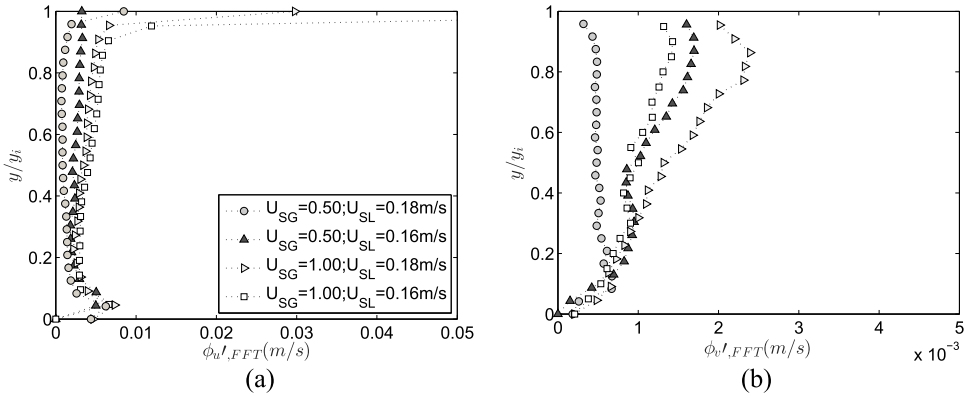

FIG. 18. Eigenfunctions of 6 Hz waves. (a) Streamwise. (b) Wall normal.

IV. CONCLUSION

The concepts of shadow technique, particle image velocimetry, controlled disturbances, and phase-locked image acquisitions were applied to investigate the evolution of interfacial waves in a turbulent gas-liquid stratified flow. The obtained experimental results show high degree of reproducibility which enabled to track the evolution of excited disturbances along the pipe. Measurements were carried out at flow rates close to the transition from smooth stratified to wavy stratified. The results reported here can help to shed some additional light on how the two-phase stratified pipe flow compares with other two-phase shear flows such as boundary layer and channel flows.

The work focused on the characterization of interfacial waves within the linear regime of their development. Therefore, only waves with very small amplitudes were investigated. The amplitude threshold for assuming waves to be within the linear regime was obtained experimentally. Preliminary tests with waves excited with different initial amplitudes allowed us to estimate qualitatively the amplitude threshold for linear regime of wave development. Within the range of tested parameters, amplitudes smaller than 1.5% of the pipe diameter displayed features of linear waves. It is important to mention that no clear and well-defined threshold was observed. The limiting amplitude was taken from the worst situation observed, when non-linear features were first observed in the experiments. For the majority of tested situations, this threshold was very conservative. Nevertheless, no significant harmonics and subharmonics were noticed in the signal spectra for waves with amplitudes smaller than 1.5% of the pipe diameter. In addition, the mean liquid height was unaffected by the presence of waves with small amplitude.

Another interesting result observed in the experimental data was the rather linear phase evolution of the interfacial waves. According to the current findings, no evident influence of turbulence in the liquid and gas phases was observed. The results clearly showed that dispersion characteristics of the waves remained unaffected even in the presence of highly noisy environment. It is also worth to mention that the same statement might not be true for highly sheared flows, i.e., high gas flow rates. A comparison of measured wave celerities against different linear models showed that linear wave theories based on finite depth are in better agreement with the experiments. Furthermore, most finite depth models displayed similar results, suggesting a weak influence of surface tension and gas density on the wave speed.

Amplification of the disturbances was measured and a monotonic exponential growth was observed for waves excited with a frequency of 4 Hz. Waves with a frequency of 6 Hz displayed a completely different behavior and no clear evidence of exponential growth or decay was traced. This result is rather interesting and suggests that small variation on the wave scale can induce severe modifications on the phenomenon. According to the experimental findings, the behavior is apparently linked to boundary layer separation of the gas flow over the liquid interface. The mechanism might be somehow similar to those observed in the recent wok of Buckley and Veron (2016). However, this conjecture still lacks of experimental support and further investigations are needed.

The part of the eigenfunctions of the interfacial waves was extracted from the flow fluctuations within the liquid layer. To the best knowledge of the authors, this is the first time that such data are reported in the literature regarding gas-liquid pipe flow. The profiles show that interfacial modes are nearly independent of inner modes for the range of the current investigation. The results are in qualitative agreement with the works of Kaffel and Riaz (2015) and Barmak *et al.* (2016), even though the flow regime is different. For low levels of liquid or for pipes with small diameters, the situation might be modified and interaction between modes can play a role.

ACKNOWLEDGMENTS

This work was supported by Petrobras from Brazil, via Grant No. 2013/00068-4, and the Akademia Program at the University of Oslo.

Andreussi, P., Asali, J. C., and Hanratty, T. J., "Initiation of roll waves in gas-liquid flows," AIChE J. **31**(1), 119–126 (1985).

Andritsos, N. and Hanratty, T. J., "Interfacial instabilities for horizontal gas-liquid flows in pipelines," Int. J. Multiphase Flow **13**, 583–603 (1987).

Ansari, M. R. and Shokri, V., "Numerical modeling of slug flow initiation in a horizontal channels using a two-fluid model," Int. J. Heat Fluid Flow **32**(1), 145–155 (2011).

Ayati, A. A., Kolaas, J., Jensen, A., and Johnsonvre, G. W., "A PIV investigation of stratified gas-liquid flow in a horizontal pipe," Int. J. Multiphase Flow **61**, 129–143 (2014).

Ayati, A. A., Kolaas, J., Jensen, A., and Johnson, G. W., "Combined simultaneous two-phase PIV and interface elevation measurements in stratified gas/liquid pipe flow," Int. J. Multiphase Flow **74**, 45–58 (2015).

Ayati, A. A., Kolaas, J., Jensen, A., and Johnson, G. W., "The effect of interfacial waves on the turbulence structure of stratified air/water pipe flow," Int. J. Multiphase Flow **78**, 104–116 (2016).

Bar-Cohen, A., Holloway, C., Kaffel, A., and Riaz, A., "Waves and instabilities in high quality adiabatic flow in a microgap channels," Int. J. Multiphase Flow **83**, 62–76 (2016).

Barmak, I., Gelfgat, A., Vitoshkin, H., Ullmann, A., and Brauner, N., "Stability of stratified two-phase flows in horizontal channels," Phys. Fluids **28**(4), 044101 (2016).

Barnea, D., "A unified model for predicting flow-pattern transitions for the whole range of pipe inclinations," Int. J. Multiphase Flow **13**(1), 1–12 (1987).

Barnea, D. and Taitel, Y., "Transient-formulation modes and stability of steady-state annular flow," Chem. Eng. Sci. **44**(2), 325–332 (1989).

Barnea, D. and Taitel, Y., "Kelvin-Helmholtz stability criteria for stratified flow: Viscous versus non-viscous (inviscid) approaches," Int. J. Multiphase Flow **19**(4), 639–649 (1993).

Bendiksen, K. and Espedal, M., "Onset of slugging in horizontal gas-liquid pipe flow," Int. J. Multiphase Flow **18**(2), 237–247 (1992).

Birvalski, M., Tummers, M. J., Delfos, R., and Henkes, R. A. W. M., "PIV measurements of waves and turbulence in stratified horizontal two-phase pipe flow," Int. J. Multiphase Flow **62**, 161–173 (2014).

Bontozoglou, V., "Weakly nonlinear Kelvin-Helmholtz waves between fluids of finite depth," Int. J. Multiphase Flow **17**(4), 509–518 (1991).

Buckley, M. P. and Veron, F., "Structure of the airflow above surface waves," J. Phys. Oceanogr. **46**(5), 1377–1397 (2016).

de Paula, I. B., Würz, W., Kämer, E., Borodulin, V. I., and Kachanov, Y. S., "Weakly nonlinear stages of boundary-layer transition initiated by modulated Tollmien-Schlichting waves," J. Fluid Mech. **732**, 571–615 (2013).

Fan, Z., Lusseyran, F., and Hanratty, T. J., "Initiation of slugs in horizontal gas-liquid flows," AIChE J. **39**(11), 1741–1753 (1993).

Funada, T. and Joseph, D. D., "Viscous potential flow analysis of Kelvin-Helmholtz instability in a channel," J. Fluid Mech. **445**, 263–283 (2001).

Gonzales, R. C., Woods, R. E., and Eddis, S. L., *Digital Image Processing Using Matlab*, 2nd ed. (Gatesmark Publishing, 2009), p. 1.

Havre, K., Stornes, K. O., and Stray, H., "Taming slug flow in pipelines," ABB Rev. **4**, 55–63 (2000).

Hewitt, G. F., Jayanti, S., and Hope, C. B., "Structure of thin liquid films in gas-liquid horizontal flow," Int. J. Multiphase Flow **16**(6), 951–957 (1990).

Issa, R. I. and Kempf, M. H. W., "Simulation of slug flow in horizontal and nearly horizontal pipes with the two-fluid model," Int. J. Multiphase Flow **29**(1), 69–95 (2003).

Johnson, G. W., Bertelsen, A. F., and Nossen, J., "An experimental investigation of roll waves in high pressure two-phase inclined pipe flows," Int. J. Multiphase Flow **35**(10), 924–932 (2009).

Jurman, L. A., Deutsch, S. E., and MacCready, M. J., "Interfacial mode interactions in horizontal gas–liquid flows," J. Fluid Mech. **238**, 187–219 (1992).

Kadri, U., Mudde, R. F., Oliemans, R. V. A., Bonizzi, M., and Andreussi, P., "Prediction of the transition from stratified to slug flow or roll-waves in gas–liquid horizontal pipes," Int. J. Multiphase Flow **35**, 1001–1010 (2009).

Kaffel, A. and Riaz, A., "Eigenspectra and mode coalescence of temporal instability in two-phase channel flow," Phys. Fluids **27**(4), 042101 (2015).

Kordyban, E. S. and Ranov, T., "Mechanism of slug formation in horizontal two-phase flow," J. Basic Eng. **92**(4), 857–864 (1970).

Landau, L. D. and Lifshitz, E. M., *Fluid Mechanics*, Course of Theoretical Physics (Elsevier, 1987).

Lin, P. Y. and Hanratty, T. J., "Prediction of the initiation of slugs with linear stability theory," Int. J. Multiphase Flow **12**(1), 79–98 (1986).

Mandhane, J. M., Gregory, G. A., and Aziz, K., "A flow pattern map for gas-liquid flow in horizontal pipes," Int. J. Multiphase Flow **1**(4), 537–553 (1974).

Nogueira, S., Sousa, R. G., Pinto, A. M. F. R., Riethmuller, M. L., and Campos, J. B. L. M., "Simultaneous PIV and pulsed shadow technique in slug flow: A solution for optical problems," Exp. Fluids **35**(6), 598–609 (2003).

Sanchis, A., Johnson, G. W., and Jensen, A., "The formation of hydrodynamic slugs by the interaction of waves in gas–liquid two-phase pipe flow," Int. J. Multiphase Flow **37**, 358–368 (2011).

Schmid, P. J. and Henningson, D. S., *Stability and Transition in Shear Flows*, Applied Mathematical Sciences Vol. 142 (Springer Verlag, 2001).

Schmid, P. J., Henningson, D. S., and Jankowski, D. F., "Stability and transition in shear flows. Applied mathematical sciences, Vol. 142," Appl. Mech. Rev. **55**, B57 (2002).

Soleimani, A. and Hanratty, T. J., "Critical liquid flows for the transition from the pseudo-slug and stratified patterns to slug flow," Int. J. Multiphase Flow **29**(1), 51–67 (2003).

Taitel, Y. and Dukler, A. E., "A model for predicting flow regime transitions in horizontal and near horizontal gas-liquid flow," AIChE J. **22**(1), 47–55 (1976).

Tzotzi, C. and Andritsos, N., "Interfacial shear stress in wavy stratified gas-liquid flow in horizontal pipes," Int. J. Multiphase Flow **54**, 43–54 (2013).

Ujang, P. M., Lawrence, C. J., Hale, C. P., and Hewitt, G. F., "Slug initiation and evolution in two-phase horizontal flow," Int. J. Multiphase Flow **32**(5), 527–552 (2006).

Valluri, P., Spelt, P. D. M., Lawrence, C. J., and Hewitt, G. F., "Numerical simulation of the onset of slug initiation in laminar horizontal channel flow," Int. J. Multiphase Flow **34**(2), 206–225 (2008).

Wallis, G. B. and Dodson, J. E., "The onset of slugging in horizontal stratified air-water flow," Int. J. Multiphase Flow **1**(1), 173–193 (1973).

Wetzel, J. M. and Arndt, R. E. A., "Hydrodynamic design considerations for hydroacoustic facilities: Part I—Flow quality," J. Fluids Eng. **116**(2), 324–331 (1994).